

total capacitance positive. With the neglect of higher harmonic terms, this implies

$$\left| \frac{C_{TP}}{C_{T0}} \right| \leq 1. \quad (6)$$

Suppose now in addition to the bias and pump voltage ($V_0 + V_P$), we apply a small signal voltage δv with components at signal and idling frequencies. What is the increment in charge which flows? From (1) we have

$$\delta q = C_T \delta v + \delta C_T V,$$

and

$$\delta C_T = \frac{dC_T}{dV} \Big|_{(V_0+V_P)} \delta v. \quad (7)$$

The first term in the equation for charge represents the ac charge produced by the pumped capacitance. It includes the action of the time-varying capacitance produced by the pump voltage mixing with the small voltages at signal and idling frequencies, giving rise to charge components at idling and signal frequencies. The second term represents the effect of the small signal voltages in varying the nonlinear capacitance and the resulting mixing with the large bias and pump voltages also to produce charge components at signal and idling frequencies. It is not difficult to show that this second nonlinear effect is equal in magnitude to the first.

For simplicity, let us assume a linear relationship between capacity and voltage, that is, a second order nonlinearity in the charge-voltage characteristic.

$$C_T = c_0 + cV. \quad (8)$$

Then in terms of the notation of (4) when only the bias and pump voltages are applied, the dc portion of the total capacity is

$$C_{T0} = c_0 + cV_0, \quad (9)$$

and the time-varying portion is

$$C_{TP} = cV_P.$$

In this notation, the substitution of the capacitance characteristic of (8) into (7) gives

$$\delta C_T = c\delta v, \quad (10)$$

and

$$\delta q = (C_{T0} + C_{TP})\delta v + c\delta v(V_0 + V_P) = (C_{T0} + cV_0)\delta v + 2C_{TP}\delta v. \quad (11)$$

Thus, in so far as the small signals are concerned, the nonlinear capacitor appears to have a static capacitance of ($C_{T0} + cV_0$) and a time-varying portion of $2C_{TP}$, that is, twice the value produced by the pump alone. This is the value of the equivalent time-varying capacitance C_3 used by Heffner and Wade.¹

$$C_3 = 2|C_{TP}|. \quad (12)$$

From (6) we see

$$\frac{C_3}{C_{T0}} \leq 2, \quad (13)$$

where we have compared the ac capacitance seen by the signal and idling frequencies to the static capacitance observed when only the bias and pump are applied. There is no

such limit to the ratio of pumped ac to static capacitance if *both* are measured at signal or idling frequencies.

The second question raised concerns the relationship between the definition of total capacitance C_T and incremental capacitance C_i . In the case of the incremental capacitance, we imagine that we have applied the bias voltage V_0 and the pump voltage V_P and then observe the increment in charge produced by applying a small-signal voltage δv with components at signal and idling frequencies.

$$q = \frac{df(V)}{dV} \Big|_{(V_0+V_P)} \delta v = C_i \delta v. \quad (14)$$

Here the incremental capacitance

$$C_i = \frac{df(V)}{dV} \Big|_{(V_0+V_P)} \quad (15)$$

has dc and time-varying components. In Rowe's notation²

$$C_i = \sum_{n=-\infty}^{\infty} C_n e^{in\omega_P t}. \quad (16)$$

One might wonder whether this definition included not only the effect of capacitance change at the pump frequency mixing with signal and idle voltage but also the terms due to variation in capacitance produced by the small signal and idling voltages mixing with the pump voltage, an effect which we have seen is of the same magnitude as the first. It is easy to show that the incremental capacitance approach does indeed include both effects and is identical to the total capacitance approach by returning to (7) which can be written,

$$\delta q = C_T \Big|_{(V_0+V_P)} \delta v + \left[\frac{dC_T}{dV} \Big|_{(V_0+V_P)} \delta v \right] V, \quad (17)$$

and (3), which relates C_T to the nonlinear characteristic

$$C_T = \frac{f(V)}{V}. \quad (3)$$

With this substitution for C_T (7) becomes

$$\begin{aligned} \delta q &= \frac{f(V)}{V} \Big|_{(V_0+V_P)} \delta v \\ &+ \left[\frac{df(V)}{dV} \Big|_{(V_0+V_P)} - \frac{f(V)}{V} \Big|_{(V_0+V_P)} \right] \delta v \\ &= \frac{df(V)}{V} \Big|_{(V_0+V_P)} \delta v = C_i \delta v. \end{aligned} \quad (18)$$

Thus, the two definitions are consistent. If one includes only that portion of the incremental capacitance which varies at the pump frequency C_i , one sees from (16) in Rowe's notation,²

$$|C_i| = 2|C_1|; \quad (19)$$

and from (11), (12), and (13)

$$C_3 = |C_i| = 2|C_1| = 2|C_{TP}| \leq 2C_{T0} \quad (20)$$

where, as before, C_{T0} represents the static capacitance observed when only the bias and pump voltages are applied.

H. HEFFNER
Dept. of the Navy
Office of Naval Res., Branch Office
London, England

A Tunnel-Diode Amplifying Converter*

Sufficient literature has already been presented to establish the fact that tunnel diodes appear to have a bright future as relatively low noise, low power consumption, amplifying devices.¹⁻⁴

In this note it is desired to report the results of using the tunnel diode as a mixing element rather than a single-frequency amplifying device.

In the usual microwave or VHF receiver, superheterodyne principles are most often utilized. In this system the signal is received by some form of antenna, amplified, and then transmitted to a mixer or transmitted directly to the mixer without amplification. In the mixer, the received signal and the local oscillator signal operate usually on a nonlinear variable-resistance device from which the intermediate frequency signal is then derived.

This mixer is usually quite noisy and quite lossy, the diode-noise figures being on the order of 7.0 db and the diode losses being on the order of 6.0 db.

It is very possible to place a negative-resistance amplifier before the mixer to minimize the effects of the mixer noise figure and loss; but the peculiar current-voltage (I-V) characteristic of the tunnel diode presents a much more desirable solution.⁵ The RF amplifier and variable resistance mixer can be entirely eliminated and the tunnel diode used to obtain the necessary high-gain and low-noise figure and to convert from the signal frequency down to the IF frequency.

Fig. 1 is representative of the I-V characteristic of the diode used in the experiments.

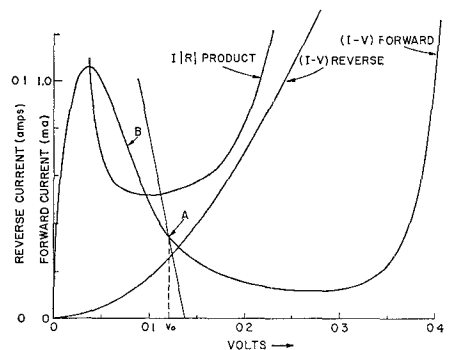


Fig. 1—Current-voltage characteristic of the germanium diode used in the calculations.

* Received by the PGMTC, October 4, 1960. This research was supported by the United States Air Force through WWRNGW of the Wright Air Dev. Div. of the Air Res. and Dev. Command.

¹ H. S. Sommers, Jr., "Tunnel diode as high-frequency devices," Proc. IRE, vol. 47, pp. 1201-1206; July, 1959.

² K. N. Chang, "Low-noise tunnel diode amplifier," Proc. IRE, vol. 47, p. 1268; July, 1959.

³ I. A. Lesk, N. Halonyak, U. S. Davidsohn, and M. W. Aarons, "Germanium and silicon tunnel diodes—design, operation, and application," 1959 WESCON CONVENTION RECORD, pt. 3, pp. 9-31.

⁴ M. E. Hines, "High-frequency negative resistance circuit principles for Esaki diode applications," Bell Sys. Tech. J., vol. 34, pp. 477-513; May, 1960.

⁵ K. N. Chang, G. H. Heilmeyer, and H. J. Prager, "Low-noise tunnel diode down converter having conversion gain," Proc. IRE, vol. 48, pp. 854-858; May, 1960.

ments. Fig. 2 is an oscilloscope presentation of the conductance of the same diode vs voltage.

The tunnel diode is used as the mixing diode, the bias adjusted for stable operation at point *A*. The total dc-source resistance (r_1) must be less than the magnitude of the negative resistance of the diode (point *B*).

The local oscillator (LO) signal is coupled into the mixer by the usual techniques. Sufficient LO drive must be supplied to modulate the tunnel diode about the $I_0 - V_0$ point. The LO is decoupled sufficiently such that it loads neither the RF nor IF circuits.

The RF equivalent circuit used to define the device parameters is shown in Fig. 3(a). Fig. 3(b) shows the equivalent circuit of the

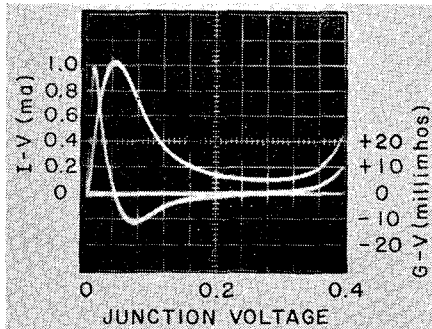


Fig. 2—Oscilloscope presentation of the conductance vs voltage characteristics of the diode used in the experiments.

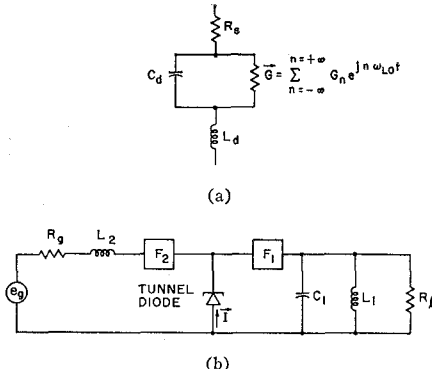


Fig. 3—(a) RF equivalent circuit of tunnel diode.
(b) Circuit of the tunnel diode mixer.

complete mixer as used in the experiments. G is the exponential Fourier series representation of the conductance waveform under local oscillator modulation. I is the exponential Fourier series representation of the diode current under LO modulation. F_2 is a band pass filter arranged in such a manner as to pass the input signals from the generator, and to act as an open circuit for the image signals. F_1 is a low-pass filter which passes the IF signals but blocks the RF input signals.

With the circuit configuration as shown in Fig. 3, let the following quantities be defined:

$$Q_2 = \frac{\omega_2(L_2 + L_d)}{R_g + R_s} \quad \bar{Q}_1 = \frac{\omega_1 C_1}{(G_1 + G_0)}$$

$$\bar{Q}_2 = \frac{\omega_2 C_d}{(G_0 + G_s + G_0)} \quad (1)$$

$$G_g + G_s = \frac{1}{(R_g + R_s)(1 + Q_2^2)} \quad (2)$$

$$\frac{G_s}{G_g} = \frac{R_s}{R_g}, \quad (3)$$

$$G_0 = -0.007 \text{ mho} \quad I_0 = 0.408 \text{ ma} \quad G_{eq0} = 0.00816$$

$$G_1 = -0.0031 \text{ mho} \quad I_1 = 0.14 \text{ ma} \quad G_{eq1} = 0.0056.$$

where

- 1) R_g is the series-source resistance and G_g is the equivalent-source conductance.
- 2) R_s is the series-loss resistance and G_s is the equivalent shunt-loss conductance.
- 3) $R_s \ll R_g$; $L_d \ll L_1$.

Using the above definitions for the equivalent conductances, the conversion power gain (W_p) may be shown to be

$$W_p = \frac{G_1 G_g}{G_1^2} \cdot \frac{4\alpha^2}{(1 - \alpha)^2}, \quad (4)$$

where

$$\alpha = \frac{G_1^2}{(G_1 + G_0)(G_g + G_s + G_0)}; \quad (5)$$

and the bandwidth (B) may be found from the following relation,

$$B = \frac{\omega_1(1 - \alpha)}{\bar{Q}_1 + \bar{Q}_2 \left(\frac{\omega_1}{\omega_2} \right)}. \quad (6)$$

The noise figure is given by

$$F = 1 + \frac{T}{T_0} \left[\frac{G_s}{G_g} + \frac{G_{eq0}}{G_g} \right. \\ \left. - \frac{G_{eq1}}{G_1} \left(\frac{G_g + G_s + G_0}{G_g} \right) \right. \\ \left. + \left(G_{eq0} + \frac{T_1}{T} G_1 \right) (G_g + G_s + G_0)^2 \right] / G_0 G_1^2, \quad (7)$$

where

T_0 = reference (source) temperature in degrees Kelvin,
 T = temperature of the diode,
 T_1 = temperature of the load,
 G_{eq0} = equivalent-noise conductance of the diode = $eI_0/2KT$,
 G_{eq1} = $e(2I_1)/2KT$.

A converter using germanium tunnel diodes has been operated at 1200 Mc. The IF frequency was 30 Mc with the local oscillator set at 1170 Mc. The diode had a peak current of 1 ma.

Several noise figure calculations were made for various points of operation about the point of maximum positive slope of the conductance curve in the negative resistance region. Best noise figures were obtained upon biasing such that V_0 is between 0.1 and 0.2 volt; this corresponds closely to the position

of minimum IR product⁶ or I/G ratio.⁷ With 50 mv of peak LO drive, moderate values of G_1 may be obtained with relatively large negative values of G_0 . The best calculated value for the noise figure was about 4.7 db, and can be obtained from the following data.

For a bias voltage of 125 mv, and a peak local oscillator voltage of 50 mv, the following parameters are obtained:

It has been assumed that the LO voltage waveform at the junction remains sinusoidal.

The series resistance, R_s , and the junction capacity are known ($R_s = 1$ ohm; $C_d = 5 \mu\text{fF}$); therefore, the equivalent-loss conductance $G_s = 0.0015$ mho. Assuming an α in (5) to be $\alpha = 0.7$, and generator conductance $G_g = 0.006$, G_1 is found to be 0.0338 mho. By (4), the gain is found to be about 26 db; assuming in (7) $T/T_0 = T_1/T = 1$, the noise figure is found to be 4.7 db. By (6) the band-pass is calculated to be about 4.0 Mc.

A block diagram of the converting system as tested is shown in Fig. 4. A ferrite

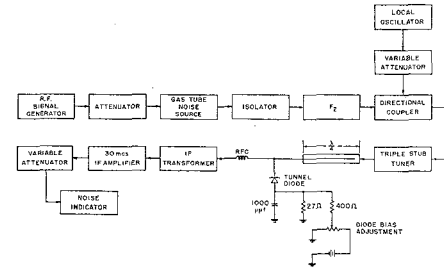


Fig. 4—Block diagram of the experimental system.

isolator was used at the input to insure good termination for the gas-tube noise source and also to isolate the converter from changes in the generator impedance (the differences in the fired and unfired condition of the noise source). F_2 is a cavity band-pass filter which, in conjunction with the triple stub tuner, acted to pass the signal but reflect the image in such a manner as to present a short circuit to the image. The directional coupler serves only the cause of LO injection with good decoupling (≈ 25 db). The quarter-wave section shown serves not only to pass the signal, but also to block the IF. The IF transformer changes the IF impedance (50 ohms) to the desired value of about 30 ohms.

With the system adjusted as described, it was a relatively easy task to bring the measured noise figure within the range of 6-8 db. By fine adjustments of the tuning on the RF side, the bias point, the local oscillator drive, the noise figure was brought within the range of the calculated value. With the noise figure brought down to about 4.5 db the measured bandwidth was about 4.0 Mc. The

⁶ K. K. N. Chang, "The optimum noise performance of tunnel diode amplifiers," Proc. IRE, vol. 48, pp. 107-108; January, 1960.

⁷ J. J. Tieman, "Shot noise in tunnel diode amplifiers," Proc. IRE, vol. 48, pp. 1418-1423; August, 1960.

signal generator was used to measure the bandwidth and also to insure the absence of image response and other spurious responses that might cause erroneous noise figure indications.

An unexpected result of this fine tuning of the system was the realization of noise figures better than that calculated. Additional fine tuning of the input impedance, diode bias, and local oscillator drive gave rise to a measured noise figure of approximately 3 db and a bandwidth of 1-2 megacycles. This condition realized very high conversion gain and was not extremely stable.

There remains now a question of relative merit of the tunnel diode converter vs the tunnel-diode amplifier followed by a standard converter. There is no generalization that can apply. The question must be resolved for each separate application, since each application will have a different set of rules governing stability, gain, bandwidth, over-all noise figure and so forth. As has been pointed out,⁸ the noise figure of the converter is in general higher than that of the amplifier. As can be seen from (4)-(7), as the gain is made very large the term $(G_g + G_s + G_0)$ becomes very small and the noise-figure equation reduces to that which applies to the one-port negative conductance amplifier. If the high-gain converter is used the system noise figure may approach or surpass that of the system using the negative conductance amplifier, for in the process of converting from signal to IF there is no loss diode mixer involved.

L. E. DICKENS
C. R. GNEITING
Radiation Lab.

The Johns Hopkins University
Baltimore, Md.
Formerly with Bendix Radio Div.
Bendix Corp.
Towson, Md.

⁸ D. J. Breitzer, "Noise figure of tunnel diode mixer," *PROC. IRE*, vol. 48, pp. 935-936; May, 1960.

Impedance Matching by Charts*

In a previous correspondence, Somlo¹ sought to rectify a misstatement in an article by Hudson,² by showing a Smith Chart method of matching impedances. The method entailed finding the correct line length of the right characteristic impedance that would match two arbitrary impedances. The method Somlo shows is substantially that given in various texts,^{3,4} although in the

texts it is done with rectangular transmission line charts rather than with Smith Charts. Indeed, for this application, the rectangular transmission line chart offers advantage over the Smith Chart. With the rectangular transmission line chart one can find the needed line length directly without having to replot the impedances and draw a second circle, as with the Smith Chart in this application as put forth by Somlo.

The statement of Somlo, "If this circle lies fully within the Smith Chart, the question has a solution, otherwise not,"¹ can be modified. What one can say is that if the circle does not lie fully within the Smith Chart (or fully in the right half plane of a rectangular impedance chart) then the impedances cannot be matched with a single length of line. In this case the thing to do is to place a third impedance on the chart so that circles between it and the first two impedances will lie fully in the domain of positive resistances (right half plane of the rectangular impedance chart or within the Smith Chart). Then the first two impedances can each be matched to the third. This will involve a matching transformer of two sections which for the correct choice of the intermediate impedance will have a wider band than a transformer of one section.⁵ Even broader band transformers could be made by increasing the number of intermediate impedances and, hence, the number of matching sections. It is possible that for certain values of mismatched impedance more than one additional intermediate impedance will have to be inserted.

MICHAEL R. LEIBOWITZ
Radio Receptor Co. Inc.
Advanced Dev. Lab.
Westbury, L. I., N. Y.

⁵ LePage and Seeley, *op cit.*, pp. 347-348.

Theoretical Evaluation of Resonance Frequencies in a Cylindrical Cavity with Radial Vanes*

When the walls of a cavity resonator are altered from a simple geometrical configuration by a small amount, the effect on the resonance frequencies can be determined by applying perturbation methods involving the use of plausible trial fields.

The case of radial vanes inserted into a cylindrical cavity poses a relatively difficult problem, especially when the vane penetration is large. The calculation of the perturbation usually involves a volume integral over the volume enclosed between the perturbed surface and the unperturbed surface¹ (or a surface integral that reduces to a similar volume integral²). The volume thus enclosed,

in the case of vanes assumed to be infinitesimally thin, is also infinitesimally small. Since the fields being integrated over the volume are finite, the integral would be infinitesimally small and thus would not represent the effect of the perturbation correctly.

An alternative approach has been worked out and has been tried out in detail for the case of lower-order modes in a shallow cylindrical cavity, perturbed by a pair of radial vanes. Good agreement between calculated and experimental values has been obtained up to changes of 28 per cent between perturbed and unperturbed frequencies.

Basically, the analysis proceeds by first dividing the cavity into different regions by an assumed cylindrical surface, passing through the inner edges of the vanes (Fig. 1). A plausible field distribution at this surface, for the *E* field, *e.g.*, and a plausible value for the resonance frequency are assumed. The electromagnetic field in two regions on opposite sides of the surface (regions 1 and 2) is built up by appropriately summing up the field distribution associated with the orthogonal modes in a simple cylindrical cavity. (It is to be noted that in these expressions the frequency is also involved.)

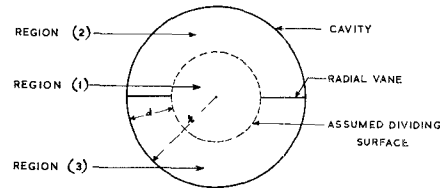


Fig. 1—Diagram showing cross section of the cavity and illustrating the method of analysis.

The Fourier components of the assumed distribution at the dividing surface are used in arriving at the above summation. For region 1 the Fourier components are so chosen that the assumed distribution is obtained for the entire range of azimuthal variation from 0 to 2π . For region 2, a different set of components is chosen so that the assumed distribution is obtained only across region 2, but the *E* field is zero at the location of the vanes for all the modes. It is to be noted that unlike some of the other perturbation methods, the boundary conditions are satisfied by the trial fields at the perturbed surface also. This makes the method applicable to cases of large vane penetration.

Since the assumed distribution and frequency are only first approximations, the *H* fields obtained in regions 1 and 2 will not be continuous across the dividing surface. An iterative procedure has been developed by which better approximations to the frequency and the assumed field distribution are obtained in successive alternate steps, while working towards continuity of *H* field. The matching of fields across the dividing surface need be done in detail only for regions 1 and 2. The matching across region 1 and region 3 follows from symmetry considerations.

In the first step in the iteration, a better approximation to the frequency is obtained

* Received by the PGMAT, October 10, 1960.

¹ P. I. Somlo, "A logarithmic transmission line chart" (Correspondence), *IRE TRANS. ON MICROWAVE THEORY AND TECHNIQUES*, vol. MTT-8, p. 463; July, 1960.

² A. C. Hudson, "A logarithmic transmission line chart," *IRE TRANS. ON MICROWAVE THEORY AND TECHNIQUES*, vol. MTT-7, pp. 277-281; April, 1959.

³ J. C. Slater, "Microwave Transmission," McGraw-Hill Book Co., Inc., New York, N. Y., p. 51; 1942.

⁴ W. R. LePage and S. Seeley, "General Network Analysis," McGraw-Hill Book Co., Inc., New York, N. Y., p. 347; 1952.

* Received by the PGMAT, October 10, 1960.

¹ J. C. Slater, "Microwave Electronics," D. Van Nostrand Co., Inc., New York, N. Y., p. 81; 1950.

² A. D. Berk, "Variational principles for electromagnetic resonators and waveguides," *IRE TRANS. ON ANTENNAS AND PROPAGATION*, vol. AP-4, pp. 104-111; April, 1956.